The magnetic field of current-carrying polygons: An application of vector field rotations

Matthew I. Grivich, and David P. Jackson

Citation: American Journal of Physics **68**, 469 (2000); doi: 10.1119/1.19461
View online: https://doi.org/10.1119/1.19461
View Table of Contents: http://aapt.scitation.org/toc/ajp/68/5
Published by the American Association of Physics Teachers

The magnetic field of current-carrying polygons: An application of vector field rotations

Matthew I. Grivich and David P. Jackson
Santa Clara University, Santa Clara, California 95053

(Received 21 May 1999; accepted 5 October 1999)

We calculate the magnetic field around a current loop consisting of a regular *N*-sided polygon by successively rotating the field obtained from a straight, finite, current-carrying wire. This involves developing and applying a vector field rotation operator, which transforms vector fields the way a rotation matrix transforms scalar fields. Using this result, we explore the various magnetic field components about the current loop and notice an interesting structure that results from the geometry of the polygons. The magnetic field on the axis of the current loop as well as the field at all points around a circular loop are considered as limiting cases.

I. INTRODUCTION

A standard calculation that often appears in an introductory physics course is the magnetic field due to a constant current flowing through a finite length of wire.[1] Students are then asked in homework problems to find the magnetic field of a current arrangement at some point of symmetry, such as the center of a square or a circle. Even in more advanced treatments of electromagnetism,[2] students are not usually asked to calculate the magnetic field at an arbitrary point about these configurations, presumably due to the difficulty of the calculations involved. In fact, it is often not until graduate school that a student finally witnesses the full calculation of the magnetic field due to a circular current loop.[3,4] The approach used here is conceptually not much more difficult than the calculation for a finite wire, thus providing a relatively straightforward, albeit somewhat tedious, method for obtaining the field of a current-carrying polygon or circle.

We begin with the magnetic field due to a finite length of wire. This is written most simply as

$$B=\frac{\mu_0 i}{4\pi d}(\sin\alpha_2-\sin\alpha_1), \tag{1}$$

with a direction given by the right-hand rule. Here, i is the current, d is the length of the perpendicular segment from the axis of the wire to the observation point P, and α_1 and α_2 are the angles formed between this perpendicular segment and lines drawn from the observation point to the ends of the wire. This is shown in Fig. 1. If the length of the current segment is taken to be $2a$ and we orient it parallel to the y axis with its center a distance R along the x axis (see Fig. 1), Eq. (1) becomes

$$\mathbf{B}=\frac{\mu_0 i}{4\pi d}\left(\frac{y+a}{\sqrt{d^2+(y+a)^2}}-\frac{y-a}{\sqrt{d^2+(y-a)^2}}\right)\times\left(\frac{z}{d}\hat{\mathbf{e}}_x-\frac{x-R}{d}\hat{\mathbf{e}}_z\right), \tag{2}$$

where $d=\sqrt{(x-R)^2+z^2}$, and the direction of the field is now explicitly written.

II. MAGNETIC FIELD DUE TO CURRENT LOOPS OF REGULAR POLYGONS

To obtain the magnetic field of a current loop in the shape of an *N*-sided polygon, we simply need to add up the contributions from N different current segments arranged in the shape of a regular polygon. To sum the fields in a straightforward manner, imagine introducing a new coordinate system, $x'y'$, that is rotated by an angle $\theta=2\pi/N$ with respect to the xy system. This will place the second segment of the polygon in an identical position in the primed coordinate system as the first segment is in the unprimed coordinate system. Thus, the magnetic field of this new segment will be given by Eq. (2), with $x\rightarrow x'$, $\hat{\mathbf{e}}_x\rightarrow\hat{\mathbf{e}}_{x'}$, $y\rightarrow y'$, etc. That is, the field of the second segment will look identical in the primed coordinate system to the field of the first segment in the unprimed system. Similarly, one can imagine a set of N coordinate systems rotated by angles $\theta_n=2\pi n/N$ (for $0\leqslant n\leqslant N-1$), each of which gives rise to an identical formula for the magnetic field in reference to a different coordinate system. The total magnetic field would then be just the sum of these,

$$\mathbf{B}_{\text{tot}}=\mathbf{B}+\mathbf{B}'+\mathbf{B}''+\cdots+\mathbf{B}''^{\cdots\prime}, \tag{3}$$

where the final term (with $N-1$ primes) refers to the magnetic field of the Nth segment in the Nth coordinate system. Of course, since this result references N different coordinate systems, it is not all that useful in this form. Therefore, we must rotate each term in Eq. (3) so that they all refer to the same coordinate system. This is more subtle than it sounds because it involves rotating a vector field. Although this sounds simple, the traditional ''coordinate system rotation'' does not completely accomplish this task. Because this topic is not typically covered in undergraduate texts,[5] we will give a fairly detailed description in the following subsections.

A. Rotating a scalar field

To begin, let us consider a coordinate system, $x'y'z'$, that has been rotated about the z axis by an angle θ with respect to a second coordinate system, xyz. The relationship between points in the primed system, $\mathbf{x}'$, and those in the unprimed system, $\mathbf{x}$, is given by $\mathbf{x}'=\mathcal{R}\mathbf{x}$, where

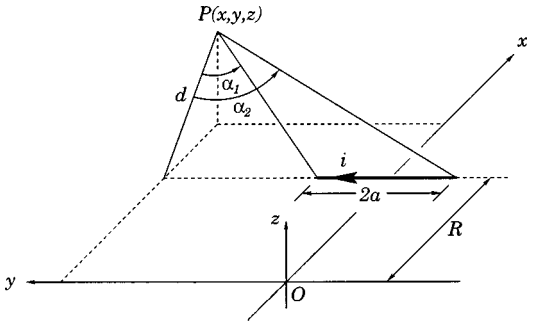

Fig. 1. A finite wire segment with constant current i is shown with an appropriate coordinate system. The magnetic field of this segment is given by Eq. (1), where use of the right-hand rule is implied, and also in Cartesian coordinates by Eq. (2).

$$\mathcal{R}\begin{pmatrix} \cos\theta & \sin\theta & 0 \\ -\sin\theta & \cos\theta & 0 \\ 0 & 0 & 1 \end{pmatrix} \tag{4}$$

is the matrix representing rotations about the z axis. The first thing we would like to consider is what happens to a scalar function under this ''coordinate system rotation.'' For example, given the function $\psi(\mathbf{x})$, what does $\psi(\mathbf{x}')=\psi(\mathcal{R}\mathbf{x})$ look like? The answer is that $\psi(\mathbf{x}')$ looks exactly the same in the primed coordinates as $\psi(\mathbf{x})$ does in the unprimed coordinates.[6] In other words, viewed in the *unprimed* coordinate system, $\psi(\mathcal{R}\mathbf{x})$ is rotated about the z axis by an angle θ with respect to $\psi(\mathbf{x})$.

That this is true is most easily seen by considering a specific example. If we let $\psi(\mathbf{x})=x$, this leads to the rotated function $\psi(\mathcal{R}\mathbf{x})=x\cos\theta+y\sin\theta$. To determine how the function has been altered, consider the ''equipotentials'' $\psi(\mathbf{x})=b$, where b is a constant. Clearly, $\psi(\mathbf{x})$ is constant on the lines $x=b$. We can infer the behavior of $\psi(\mathcal{R}\mathbf{x})$ by asking, ''what are the equipotentials of $\psi(\mathcal{R}\mathbf{x})$?'' In this case, they are found by solving $x\cos\theta+y\sin\theta=b$, which gives $y=-x\cot\theta+b\csc\theta$. A straightforward check reveals that this is indeed the equation of the line $x=b$ after it has been rotated counterclockwise about the z axis by an angle θ. This implies, as we claimed earlier, that $\psi(\mathbf{x}')$ looks the same in the primed coordinates as $\psi(\mathbf{x})$ does in the unprimed coordinates.[7]

B. Moving and spinning a vector field

Next, let us consider what happens to a vector function, $\mathbf{A}(\mathbf{x})$, subjected to a coordinate rotation, $\mathbf{x}'=\mathcal{R}\mathbf{x}$. Although it is tempting to say that $\mathbf{A}(\mathbf{x}')$ looks identical in the primed system as $\mathbf{A}(\mathbf{x})$ looks in the unprimed system, this is not the case. Since each component of $\mathbf{A}(\mathbf{x})$ is a scalar function, we have

$$\mathbf{A}(\mathcal{R}\mathbf{x})=A_x(\mathcal{R}\mathbf{x})\hat{\mathbf{e}}_x+A_y(\mathcal{R}\mathbf{x})\hat{\mathbf{e}}_y+A_z(\mathcal{R}\mathbf{x})\hat{\mathbf{e}}_z. \tag{5}$$

Viewed in the unprimed coordinates, each of the transformed scalar functions in Eq. (5) has been rotated by an angle θ with respect to the original functions. Notice, however, that the unit vectors have not changed. This means the components of each transformed vector are exactly the same as the components of the original vector. To put it another way, the vector itself has not changed, it has simply moved to a new (rotated) position. Thus, a coordinate rotation does not result in a true rotation of a vector field.

Let us extend our previous example and consider the vector field $\mathbf{A}(\mathbf{x})=x\hat{\mathbf{e}}_x$. This function has all vectors pointing in the $\pm x$ direction. In addition, each of the ''equifield'' lines, $x=b$, contains vectors with the same magnitude and direction. The scalar function, $A_x(\mathbf{x})=x$, rotates to give $\mathbf{A}(\mathbf{x}')=\mathbf{A}(\mathcal{R}\mathbf{x})=(x\cos\theta+y\sin\theta)\hat{\mathbf{e}}_x$, and hence the new equifield lines are described by $y=-x\cot\theta+b\csc\theta$. Not surprisingly, the equifield lines have been rotated exactly the same way as in the previous example. Note, however, that these vectors are still pointing in the $\pm x$ direction. To accomplish a true rotation of the vector field requires that we *spin* the vectors by an angle θ in addition to rotating their positions.

To spin the vectors, we appeal to the rotation matrix once again and consider $\mathbf{A}'(\mathbf{x})=\mathcal{R}\mathbf{A}(\mathbf{x})$. This will spin every vector in a direction opposite to that of a function under a coordinate rotation $\mathbf{x}'=\mathcal{R}\mathbf{x}$.[8] Since we want to spin the vectors in the same direction as their positions rotate, we must transform according to $\mathbf{A}'(\mathbf{x})=\mathcal{R}(-\theta)\mathbf{A}(\mathbf{x})=\mathcal{R}^{-1}(\theta)\mathbf{A}(\mathbf{x})$. For an arbitrary vector field, the transformed components are then given by $(A_x',A_y',A_z')=(A_x\cos\theta-A_y\sin\theta,A_x\sin\theta+A_y\cos\theta,A_z)$. Returning once again to our example, $\mathbf{A}(\mathbf{x})=x\hat{\mathbf{e}}_x$, we have $(A_x',A_y',A_z')=(x\cos\theta,x\sin\theta,0)$. This new vector field still has equifield lines given by $x=b$, indicating that the locations of the vectors have not changed. The components of these vectors, however, are given by $(b\cos\theta,b\sin\theta)$, demonstrating that they have been spun by an angle θ, as desired.

C. Rotating a vector field

In the last two subsections, we have seen that the rotation matrix $\mathcal{R}$ can be applied to a vector field in two different ways. Rotating the positions of the vectors by an angle θ is carried out with a coordinate transformation $\mathbf{x}'=\mathcal{R}\mathbf{x}$, and spinning the vectors by an angle θ is accomplished via $\mathbf{A}'=\mathcal{R}^{-1}\mathbf{A}$. Rotating a vector field is then achieved by combining these two operations, which defines a vector field rotation operator, $\mathfrak{R}(\theta)$, by[9]

$$\mathbf{A}'(\mathbf{x}')=\mathcal{R}\{\mathbf{A}(\mathbf{x})\}\equiv\mathcal{R}^{-1}\mathbf{A}(\mathcal{R}\mathbf{x}). \tag{6}$$

Equation (6) is valid for rotations about any axis provided the rotation matrix is changed accordingly. For rotations about the z axis, the component functions are given by[10]

$$\begin{aligned} A_x'&=\cos\theta\,A_x(x\cos\theta+y\sin\theta,-x\sin\theta+y\cos\theta,z) \\ &\quad-\sin\theta\,A_y(x\cos\theta+y\sin\theta,-x\sin\theta+y\cos\theta,z), \\ A_y'&=\sin\theta\,A_x(x\cos\theta+y\sin\theta,-x\sin\theta+y\cos\theta,z) \\ &\quad+\cos\theta\,A_y(x\cos\theta+y\sin\theta,-x\sin\theta+y\cos\theta,z), \\ A_z'&=A_z(x\cos\theta+y\sin\theta,-x\sin\theta+y\cos\theta,z). \end{aligned} \tag{7}$$

Using our example function one last time, the rotated components of $\mathbf{A}(\mathbf{x})=x\hat{\mathbf{e}}_x$ are given by $A_x'=(x\cos\theta+y\sin\theta)\cos\theta$, $A_y'=(x\cos\theta+y\sin\theta)\sin\theta$, and $A_z'=0$. As before, the equifield lines are given by $y=-x\cot\theta+b\csc\theta$, indicating that the positions have been rotated. In addition, the components of the vectors on these lines are

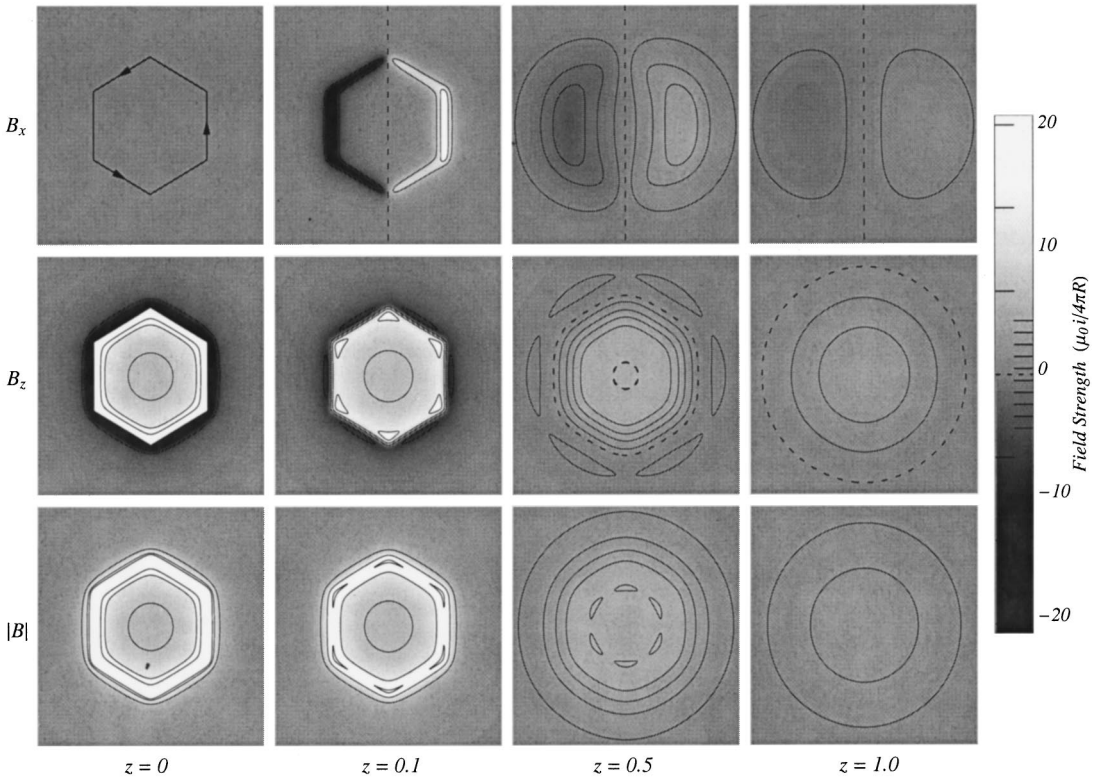

Fig. 2. Contour plots of B_x, B_z, and $|B|$ for the hexagonal current loop shown in the upper left corner. (Note that $B_x=0$ everywhere in the xy plane.) The field strength is indicated by shading as shown on the color scale and is the same for all graphs. In contrast, two different sets of contour lines (superimposed on the color scale) are used, one for the $z=0$ and $z=0.1$ graphs, and another, with a spacing about seven times smaller, for the $z=0.5$ and $z=1$ graphs (Ref. 12).

$(b\cos\theta, b\sin\theta, 0)$, illustrating that they have been spun as well.

D. Application to magnetic fields

Armed with this vector field rotation operator, each term in Eq. (3) can now be written in terms of a single coordinate system. The result is

$$\mathbf{B}_{\text{tot}}(\mathbf{x})=\sum_{n=0}^{N-1}\mathfrak{R}_n\{\mathbf{B}(\mathbf{x})\}=\sum_{n=0}^{N-1}\mathcal{R}_n^{-1}\mathbf{B}(\mathcal{R}_n\mathbf{x}), \tag{8}$$

where the subscript n designates a rotation angle of $\theta_n=2\pi n/N$. This formula sums the magnetic field contributions from N current-carrying segments of a regular polygon centered at the origin. The field of a single segment of a polygon is obtained from Eq. (2) by including a geometric constraint between the length of a segment and the ''radius'' of the polygon given by $a=R\tan(\pi/N)$. Inserting this single-segment field into Eq. (8) yields the final result,

$$\mathbf{B}_{\text{tot}}=\sum_{n=0}^{N-1}\frac{\mu_0 i}{4\pi R}\left[\frac{\tan(\pi/N)+(x\sin\theta_n-y\cos\theta_n)}{H_+}+\frac{\tan(\pi/N)-(x\sin\theta_n-y\cos\theta_n)}{H_-}\right]\times\frac{z\cos\theta_n\hat{\mathbf{e}}_x+z\sin\theta_n\hat{\mathbf{e}}_y+(1-x\cos\theta_n-y\sin\theta_n)\hat{\mathbf{e}}_z}{(1-x\cos\theta_n-y\sin\theta_n)^2+z^2}, \tag{9}$$

where

$$H_\pm=\sqrt{r^2+\sec^2(\pi/N)-2(x\cos\theta_n+y\sin\theta_n)\pm 2(x\sin\theta_n-y\cos\theta_n)\tan(\pi/N)} \tag{10}$$

are the distances from the observation point to the ends of the wire segments and $r=\sqrt{x^2+y^2+z^2}$ is the distance of the observation point from the origin. Here, and for the remainder of this paper, we use dimensionless coordinates x, y, and z that have been scaled by the radius of the polygon, R.[11]

Equations (9) and (10) represent the exact result for the magnetic field of a current loop in the shape of a regular, N-sided polygon centered at the origin. Unfortunately, since each term in the sum is equally important, this result is not very convenient for analytic calculations. However, modern numerical analysis programs such as Mathematica or Maple can handle equations such as these with relative ease. As an example, Fig. 2 shows a series of constant z contour plots of B_x, B_z, and $|B|$ for a hexagon. In this figure, lighter regions represent larger (positive) values and darker regions correspond to smaller (or more negative) values. Because subtle

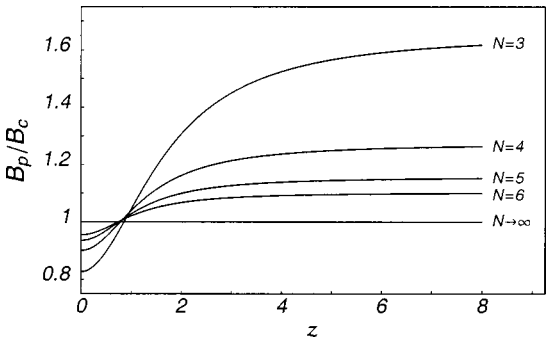

Fig. 3. The ratio of the on-axis field of a polygon to that of a circle for $3 \leqslant N \leqslant 6$. These curves have a value of $(N/\pi)\sin(\pi/N)$ at $z=0$ and approach $(N/\pi)\tan(\pi/N)$ as $z\to\infty$ as described in the text.

features of the field are difficult to discern by relying solely on the coloring scheme, we have included some contour lines on these graphs. Since the range of field values decreases dramatically for increasing z, we have used two different sets of equally spaced contour lines, one for the $z=0$ and $z=0.1$ plots, and another, with a spacing about seven times smaller, for the $z=0.5$ and $z=1.0$ plots.[12] These two sets of contour lines are superimposed on the color scale.

A surprising feature in this figure is the appearance of ''islands'' of local maxima and minima in the B_z and $|B|$ plots. This behavior is present in all polygons, but becomes less and less pronounced as N increases. Explaining exactly why these islands appear will challenge even the brightest students. Because of these extrema, it can be a bit confusing to try and match up the contour lines on the graphs with those on the color scale. For example, there are six curves on the graph of $|B|$ for $z=0$ even though the color scale shows only three positive contour lines. This is because there is a maximum (on top of the wire) on this graph that results in two contour lines for each of the magnetic field values chosen. Also, it is worth mentioning that the outermost curves on the graphs of $|B|$ for $z=0.5$ and $z=1$ correspond to the smallest positive contour line on the color scale.

III. SPECIAL CASES

A. On the axis

The magnetic field on the z axis of the current loop is easily found by setting $x=y=0$ in Eq. (9) to get

$$\mathbf{B}_p=\sum_{n=0}^{N-1}\frac{\mu_0 i}{4\pi R}\frac{2\tan(\pi/N)}{\sqrt{\sec^2(\pi/N)+z^2}}\times\left(\frac{z\cos\theta_n\hat{\mathbf{e}}_x+z\sin\theta_n\hat{\mathbf{e}}_y+\hat{\mathbf{e}}_z}{1+z^2}\right). \tag{11}$$

The x and y terms sum to zero by symmetry and each of the z terms are identical, giving

$$\mathbf{B}_p=\frac{\mu_0 i}{4\pi R}\frac{2N\tan(\pi/N)}{\sqrt{\sec^2(\pi/N)+z^2}}\left(\frac{1}{1+z^2}\right)\hat{\mathbf{e}}_z. \tag{12}$$

It is instructive to compare this result to the magnetic field on the axis of a circular current loop, obtained by taking the limit $N\to\infty$ in Eq. (12) to get $\mathbf{B}_c=(\mu_0 i/2R)(1+z^2)^{-3/2}\hat{\mathbf{e}}_z$. Figure 3 shows the ratio of these fields, B_p/B_c, for $3\leqslant N\leqslant 6$. Notice that the on-axis fields of the polygons are smaller than that of the circle for small values of z. This reflects the fact that points on the polygons are, on average, further from the origin than points on the circle. As z is increased, the on-axis fields of the polygons become larger than that of the circle and their ratio appears to level off to a constant value. This reflects the dipole behavior of the fields for large z and the fact that the polygons have a larger area than the circle.

Quantitatively, the fields at the center of the current loops are obtained by taking $z=0$ to get $B_p/B_c=(N/\pi)\sin(\pi/N)$. The large z behavior is obtained by expanding B_p and B_c for $z\gg 1$. In this case, the fields can both be written

$$B=\frac{\mu_0}{4\pi}\frac{2iA}{(zR)^3}, \tag{13}$$

where A is the area of the current loop. Note that this is just the on-axis field of a magnetic dipole with dipole moment $m=iA$.[13] For a circle and polygon, the areas are given by $A_c=\pi R^2$ and $A_p=NR^2\tan(\pi/N)$. Thus, we see that as z increases, the ratio of the fields in Fig. 3 asymptotically approaches the ratio of their areas, $B_p/B_c\to A_p/A_c=(N/\pi)\tan(\pi/N)$.

B. A circular current loop

A more challenging calculation is to find the magnetic field at all points due to a circular current loop. This is accomplished by taking the limit $N\to\infty$ in Eq. (9). We begin by expanding to lowest order in $1/N$, which yields

$$\mathbf{B}\approx\sum_{n=0}^{N-1}\frac{\mu_0 i}{4\pi R}\times\left(\frac{z\cos\theta_n\hat{\mathbf{e}}_x+z\sin\theta_n\hat{\mathbf{e}}_y+(1-x\cos\theta_n-y\sin\theta_n)\hat{\mathbf{e}}_z}{[1+r^2-2(x\cos\theta_n+y\sin\theta_n)]^{3/2}}\right)\times\Delta\theta, \tag{14}$$

where $\Delta\theta=2\pi/N$ is the angle subtended by one segment of the polygon. In the limit $N\to\infty$, this sum becomes an integral,

$$\mathbf{B}=\frac{\mu_0 i}{4\pi R}\times\int_0^{2\pi}\frac{z\cos\theta\hat{\mathbf{e}}_x+z\sin\theta\hat{\mathbf{e}}_y+(1-x\cos\theta-y\sin\theta)\hat{\mathbf{e}}_z}{[1+r^2-2(x\cos\theta+y\sin\theta)]^{3/2}}d\theta, \tag{15}$$

giving the magnetic field of a circular current loop in terms of Cartesian coordinates.

Because of the underlying symmetry, it is appropriate to convert this result into cylindrical coordinates (ρ,ϕ,z). Substituting for the coordinates and unit vectors, defining $\omega=\phi-\theta$, and exploiting the periodicity of the trig functions, we end up with

$$\mathbf{B}(\rho,z)=\frac{\mu_0 i}{4\pi R}\int_0^{2\pi}\frac{z\cos\omega\hat{\mathbf{e}}_\rho+(1-\rho\cos\omega)\hat{\mathbf{e}}_z}{[1+\rho^2+z^2-2\rho\cos\omega]^{3/2}}d\omega. \tag{16}$$

As expected, the ϕ-component has integrated to zero. Although a bit tedious, this result can be written in terms of complete elliptic integrals,

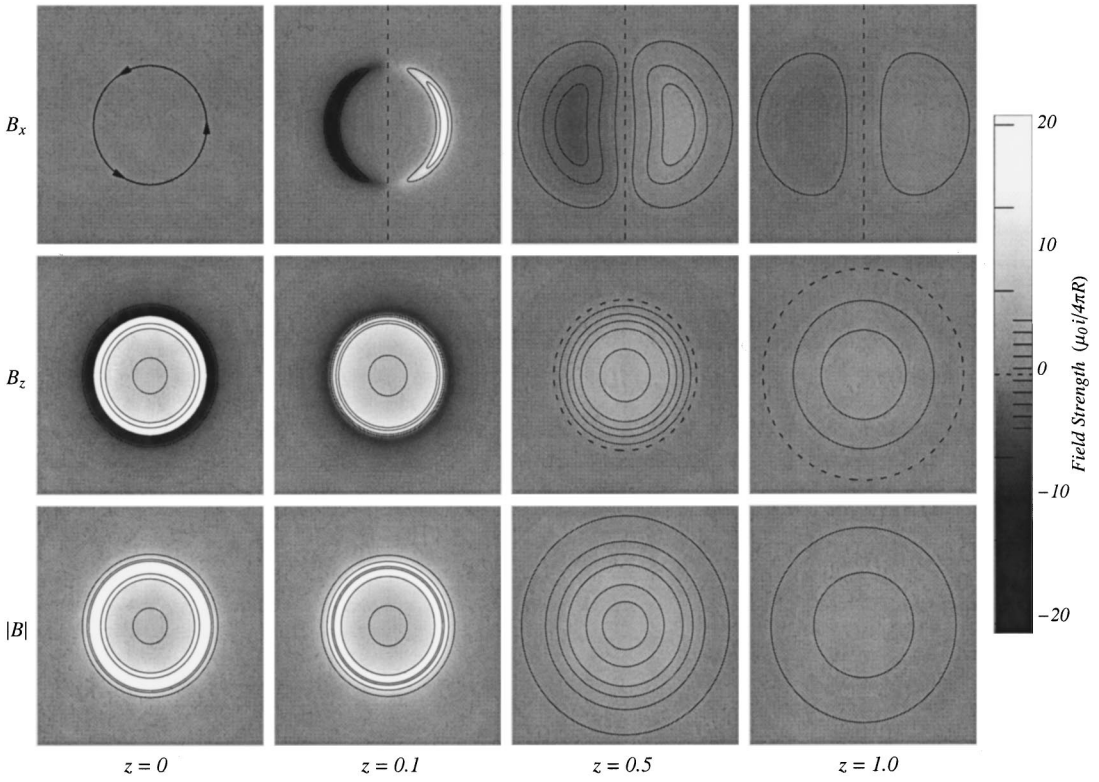

Fig. 4. Contour plots of B_x, B_z, and $|B|$ for the circular current loop shown in the upper left corner. For comparison, the same color scheme and contour lines have been used as in Fig. 2.

$$B_\rho = \frac{\mu_0 i}{4\pi R}\,\frac{2z}{\rho\sqrt{(1+\rho)^2+z^2}}\left[\frac{1+\rho^2+z^2}{(1-\rho)^2+z^2}E(k)-K(k)\right], \tag{17}$$

$$B_z = \frac{\mu_0 i}{4\pi R}\,\frac{2}{\sqrt{(1+\rho)^2+z^2}}\left[\frac{1-\rho^2-z^2}{(1-\rho)^2+z^2}E(k)+K(k)\right], \tag{18}$$

where $k=\sqrt{4\rho/[(1+\rho)^2+z^2]}$. Equations (17) and (18) represent the magnetic field due to a circular current loop of radius R centered at the origin.[4] Figure 4 shows some constant z contour plots of B_x, B_z, and $|B|$ for a circular current loop. The same shading scheme and contour lines have been used as in Fig. 2 to allow for a direct comparison. One obvious difference is that the islands of extrema that exist for polygons have coalesced into annuli for the circle. This is easily observed by referring to the graphs of $|B|$ for $z=0.1$ or $z=0.5$. In each case, the small islands in the hexagon plots have given way to an annulus (with two contours) in each of the circle plots. This is why there are more curves in some of the graphs than there are contours on the color scale. While this same behavior occurs in the B_z graphs for $z=0.1$ or $z=0.5$, the specific contour lines chosen do not necessarily reveal this behavior.

Clearly, the fields of a polygon and a circle are quite different when you are close to the loop but appear more and more alike the farther you move away. While this is not terribly surprising in light of our discussion regarding Fig. 3, we did not expect to see such a striking similarity at a distance of only one radius.

IV. CONCLUSION

We have calculated the magnetic field of a current loop in the shape of a regular, N-sided polygon centered at the origin. We obtained this result by applying a vector field rotation operator to the magnetic field of a straight, finite, current-carrying wire. This problem has a rich mixture of analytic and computational aspects that make it useful as an advanced undergraduate student project. Alternatively, it would make a nice addition to a course on electromagnetism or mathematical physics, either as part of the lectures or as the basis for a series of homework problems.

ACKNOWLEDGMENTS

We would like to thank Philip T. McCormick and the referees, whose thorough readings of this manuscript resulted in a number of positive changes.

[1]Paul A. Tipler, *Physics for Scientists and Engineers* (Worth, New York, 1991), pp. 815–825.
[2]David J. Griffiths, *Introduction to Electrodynamics* (Prentice–Hall, Englewood Cliffs, NJ, 1981), pp. 184–189.
[3]J. D. Jackson, *Classical Electrodynamics*, 2nd ed. (Wiley, New York, 1975), pp. 177–180.
[4]L. D. Landau, E. M. Lifshitz, and L. P. Pitaevskii, *Electrodynamics of Continuous Media*, 2nd ed. (Pergamon, Elmsford, 1984), p. 112.
[5]We were not able to find any texts that discussed vector field rotations. We thank one of the referees for supplying us with Refs. 9 and 10.
[6]George Arfken, *Mathematical Methods for Physicists*, 3rd ed. (Academic, San Diego, 1985) p. 264.
[7]One of the main difficulties when working with coordinate rotations is to assume that the value of the function $\psi(\mathbf{x})$ moves from $\mathbf{x}$ to $\mathcal{R}\mathbf{x}$ under the rotation. When viewed in the unprimed coordinate system, $\psi(\mathbf{x})$ is actually

replaced by $\psi(\mathcal{R}\mathbf{x})$, which means that the value $\psi(\mathcal{R}\mathbf{x})$ has moved from $\mathcal{R}\mathbf{x}$ to $\mathbf{x}$.

[8]George Arfken, *Mathematical Methods for Physicists*, 3rd ed. (Academic, San Diego, 1985), p. 201.

[9]S. S. Schweber, *An Introduction to Relativistic Quantum Field Theory* (Row, Peterson, Evanston, 1961), p. 31.

[10]J. M. Blatt and V. F. Weiskopf, *Theoretical Nuclear Physics* (Wiley, New York, 1952), p. 796.

[11]We have made the variable substitutions $x'=x/R$, $y'=y/R$, $z'=z/R$ and then dropped the primes.

[12]In general, the contours used for the B_x, B_z, and $|B|$ plots are the same. However, for $z=0.5$, the contours used on the $|B|$ plot have a *slightly* different spacing than those on the B_x and B_z plots. The difference is less than 1% and was chosen to make the local maxima visible.

[13]David J. Griffiths, *Introduction to Electrodynamics* (Prentice–Hall, Englewood Cliffs, NJ, 1981), pp. 212–213.

ANTHROPIC REASONING

This sort of reasoning is called anthropic, and it has a bad name among physicists. Although I have used such arguments myself in some of my own work on the problem of the vacuum energy, I am not that fond of anthropic reasoning. I would personally be much happier if the values of all the constants of nature could be precisely calculated on the basis of fundamental principles, rather than having to think about what values are favorable to life. But nature cares little about what physicists prefer.

Steven Weinberg, ''Before the Big Bang,'' New York Review of Books, June 12, 1997.